

**Baran Usluel**

# Mathematical Investigation

Modelling the Inverse Kinematics of a 6 DOF Articulated Robot

## Table of Contents

Introduction.....	3
Robot Configuration.....	3
Aim of Exploration.....	4
Mathematical Principles .....	5
Investigation.....	7
Determining DH Parameters .....	7
Forward Kinematics .....	8
Verification of Model.....	9
Inverse Kinematics .....	9
Verification of Inverse Kinematics .....	11
Conclusion .....	12
Works Cited .....	13

## Introduction

I have been fascinated by robots since a young age. As I grew up, I read about them and made attempts at building basic versions of them. More recently, I developed a particular interest in the theory and Mathematics that goes into designing, building, and controlling them. My extended essay is about the effects of changing the number of degrees of freedom (DOF) in robot arms on various variables, and following the same theme, my Math IA is about the calculations necessary to control them. I believe that my research is significant because developing a suitable kinematic model and using it to develop an accurate and efficient inverse kinematics solution is crucial for the practical and precise control of automated robots.

## Robot Configuration

This paper will be about articulated robots (more commonly known as robot arms, due to their human-like movements), which only have rotary joints, and no linear joints (Figure 1).

Further, the articulated robot will have 6 joints or degrees of freedom (DOF). This is because it is the most commonly used type of robot for typical industrial applications. The joint configuration of the robot will be similar to popular industrial robots such as the FANUC R-2000 (Figure 2) and the Motoman UP165, meaning that it will have a structure like that in Figure 3, with its joints rotating in the indicated directions.

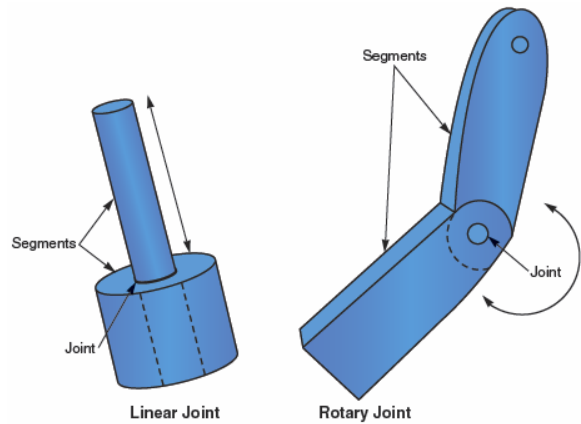


Figure 1 (Ross, Fardo and Masterson)



Figure 2, FANUC R-2000 iC/270F (FANUC)

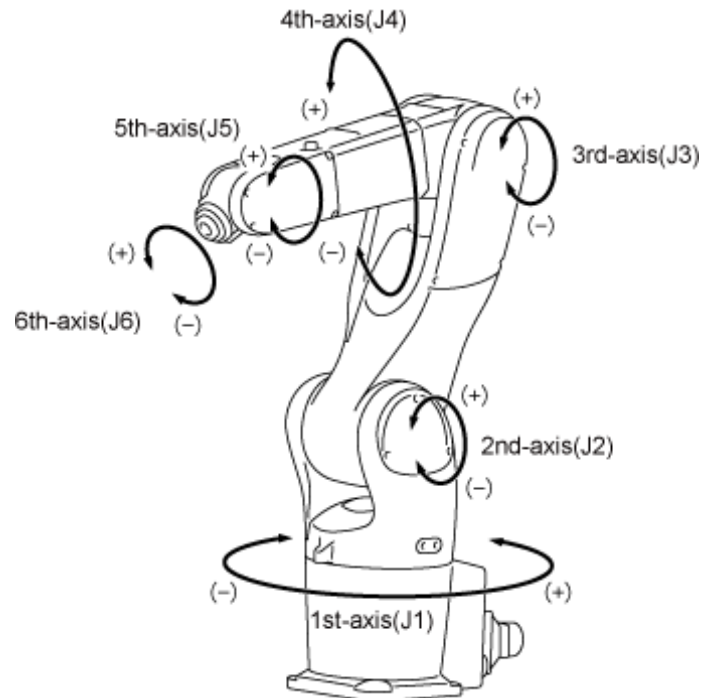


Figure 3, 6-Axis Robot Joints (DENSO WAVE INCORPORATED)

Finally, one of the most distinct features of the robot design we will be modelling is the existence of a Euler wrist. Also known as a spherical wrist, ball wrist or triple roll wrist, this is when the rotation axes of the last three joints intersect at a single location. This is displayed in Figure 4 by the intersection of  $z_3$ ,  $z_4$  and  $z_5$  which are the rotation axes of  $\theta_4$ ,  $\theta_5$  and  $\theta_6$  respectively. Simply put, this means that there is no link distance between the last three joints, and hence rotating them doesn't affect the position of the end-effector (the robot's end-point), but rather its orientation. It should be noted that in this case, the end-effector point is taken as the intersection point of these three axes. This configuration "allows for the decoupling of the position and orientation kinematics," so that an analytical solution exists and a numerical/computed approach doesn't have to be adopted. The use of the Euler wrist will mean that the model won't be universally applicable to all 6 DOF articulated robots with the same joint configuration. However, this is a limitation and assumption that is commonly utilized in literature to make the inverse kinematics solvable (Kucuk and Bingul).

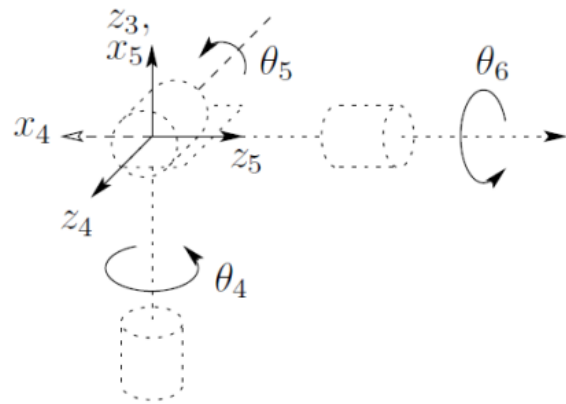


Figure 4, Euler wrist (Szabó, Budai and Kovács)

### Aim of Exploration

The aim of this investigation is to develop a mathematical model for the inverse kinematics of a 6 DOF articulated robot. Inverse kinematics is the calculation of the necessary joint angles for the end-effector to reach a target position. It is the opposite of forward kinematics, which is the calculation of the end-effector's position and orientation from the known joint angles. Inverse kinematics is a much more complex computation, because there are often an infinite number of solutions to the problem. There are two different approaches to inverse kinematics: numerical (performed by computers) and analytical methods. To make the inverse kinematics analytically solvable, we will be using a robot with a Euler wrist, which decouples the position and orientation kinematics so that only three of the six joints are responsible for each (Kucuk and Bingul).

When there are only a few DOF in the arm, the calculations can be done through simple geometry and trigonometry; however, this is not the case for robots with larger numbers of DOF, which is why I will adopt an algebraic solution using homogenous transformation matrices. This approach will be similar to what was done by Kucuk and Bingul during their research on solving the inverse kinematics of a different 6 DOF robot (the Stanford Manipulator) that has a more outdated and uncommon joint configuration.

Additionally, it should be noted that a common problem with inverse kinematics is that there are often multiple solutions or singularities; that is why the solutions yielded by the model will have to be verified by checking whether they are within the physical limits of the robot (i.e. many joints can't turn 180 degrees on themselves) and also whether they do indeed move the end-effector to the desired position (sometimes this isn't the case because of the multiple values that inverse trigonometric functions yield).

## Mathematical Principles

Firstly, the following trigonometric identities and equations will be utilized in the investigation, for simplicity:

	Equations	Solutions
1	$a \sin \theta + b \cos \theta = c$	$\theta = A \tan 2(a, b) \mp A \tan 2(\sqrt{a^2 + b^2 - c^2}, c)$
2	$a \sin \theta + b \cos \theta = 0$	$\theta = A \tan 2(-b, a)$ or $\theta = A \tan 2(b, -a)$
3	$\cos \theta = a$ and $\sin \theta = b$	$\theta = A \tan 2(b, a)$
4	$\cos \theta = a$	$\theta = A \tan 2(\mp \sqrt{1 - a^2}, a)$
5	$\sin \theta = a$	$\theta = A \tan 2(a, \mp \sqrt{1 - a^2})$

Table 1, Some trigonometric equations and solutions used in inverse kinematics (Kucuk and Bingul)

In the table above,  $A \tan 2(a, b)$  is the computer science notation for the four-quadrant inverse tangent, meaning that it is equivalent to calculating  $\arctan(a / b)$  and identifying the value which is in the correct quadrant. This expression has been used for clarity, and for compatibility with MATLAB when computing the inverse kinematics equations. Its meaning and usage has been explained here because it may be an unfamiliar notation for most readers.

Next are the homogenous transformations. These are 4x4 transformation matrices, as shown in Figure 5, that specify the position and orientation of each of the joints in space with respect to the base of the robot. They are composed of a 3x3 rotation matrix and a 3x1 translation matrix. The bottom row of the transformation matrix is always fixed as [0 0 0 1] (Yetim). We will be using homogenous transformations in this paper because they are the most commonly used representation in literature.

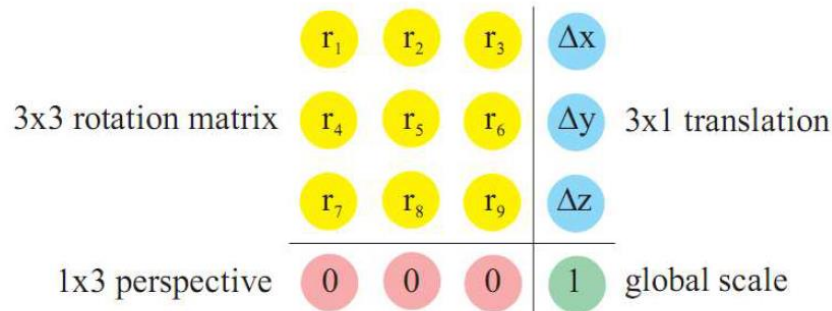


Figure 5, Homogenous transformation matrix (Yetim)

Further, we have to define our coordinate system. We will be using a right-handed, Cartesian coordinate system. When you hold your hand so that your fingers point towards the x-axis, and they can curl towards the y-axis, then your thumb will point towards the z-axis. Additionally, when we are performing rotations around the axes, we must be clear about the direction of the rotation. Therefore, when you look down the positive side of the axis, a rotation by a positive angle will be counterclockwise (Yetim).

And finally, one must be familiarized with the Denavit-Hartenberg (DH) parameters for describing robotic joint configurations. This is a standard set of parameters used in robotics, for describing the transformation between two adjacent joints. The four parameters are  $a_{i-1}$ ,  $\alpha_{i-1}$ ,  $d_i$  and  $\theta_i$ , which are the link length, link twist, link offset and joint angle, respectively. Figure 6 shows the coordinate frame assignment for a general robot, with the parameters labelled (Kucuk and Bingul).

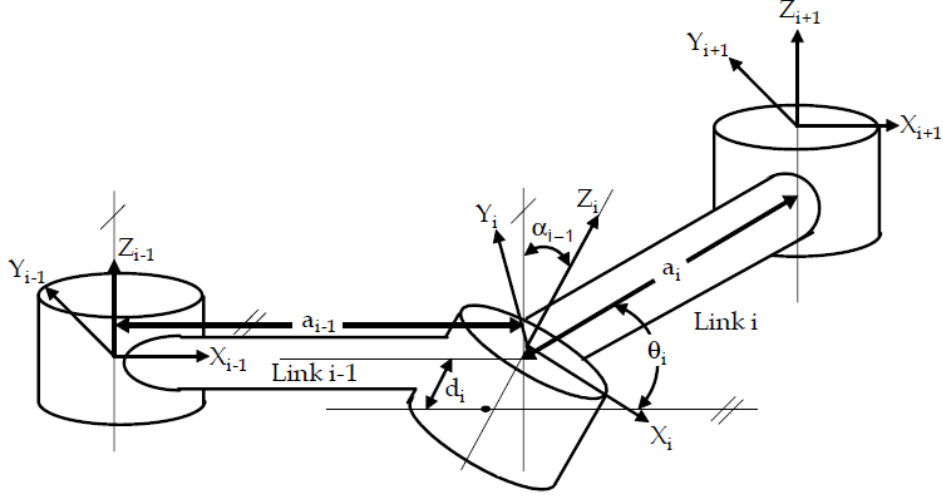


Figure 6, Coordinate frame assignment (Kucuk and Bingul)

“The distance from  $Z_{i-1}$  to  $Z_i$  measured along  $X_{i-1}$  is assigned as  $a_{i-1}$ , the angle between  $Z_{i-1}$  and  $Z_i$  measured along  $X_i$  is assigned as  $\alpha_{i-1}$ , the distance from  $X_{i-1}$  to  $X_i$  measured along  $Z_i$  is assigned as  $d_i$  and the angle between  $X_{i-1}$  to  $X_i$  measured about  $Z_i$  is assigned as  $\theta_i$ ” (Kucuk and Bingul). The transformation matrix for a link is then shown as:

$$\begin{aligned}
 {}^{i-1}T &= R_x(\alpha_{i-1})D_x(a_{i-1})R_z(\theta_i)Q_i(d_i) \\
 &= \begin{bmatrix} 1 & 0 & 0 & 0 \\ 0 & c\alpha_{i-1} & -s\alpha_{i-1} & 0 \\ 0 & s\alpha_{i-1} & c\alpha_{i-1} & 0 \\ 0 & 0 & 0 & 1 \end{bmatrix} \begin{bmatrix} 1 & 0 & 0 & a_{i-1} \\ 0 & 1 & 0 & 0 \\ 0 & 0 & 1 & 0 \\ 0 & 0 & 0 & 1 \end{bmatrix} \begin{bmatrix} c\theta_i & -s\theta_i & 0 & 0 \\ s\theta_i & c\theta_i & 0 & 0 \\ 0 & 0 & 1 & 0 \\ 0 & 0 & 0 & 1 \end{bmatrix} \begin{bmatrix} 1 & 0 & 0 & 0 \\ 0 & 1 & 0 & 0 \\ 0 & 0 & 1 & d_i \\ 0 & 0 & 0 & 1 \end{bmatrix} \\
 &= \begin{bmatrix} c\theta_i & -s\theta_i & 0 & a_{i-1} \\ s\theta_i c\alpha_{i-1} & c\theta_i c\alpha_{i-1} & -s\alpha_{i-1} & -s\alpha_{i-1} d_i \\ s\theta_i s\alpha_{i-1} & c\theta_i s\alpha_{i-1} & c\alpha_{i-1} & c\alpha_{i-1} d_i \\ 0 & 0 & 0 & 1 \end{bmatrix}
 \end{aligned} \tag{Equation 1}$$

(Kucuk and Bingul)

$R_x$  and  $R_z$  denote rotation,  $D_x$  and  $Q_i$  is translation, and  $c\theta_i$  and  $s\theta_i$  are shortened versions of  $\cos\theta_i$  and  $\sin\theta_i$ . When the transformation matrices for each of the joints are multiplied, we can find the transformation matrix of the end-effector.

$${}_{\text{end\_effector}}^{\text{base}}T = {}_1^0T {}_2^1T \dots {}_n^{n-1}T \quad {}_{\text{end-effector}}^{\text{base}}T = \begin{bmatrix} r_{11} & r_{12} & r_{13} & p_x \\ r_{21} & r_{22} & r_{23} & p_y \\ r_{31} & r_{32} & r_{33} & p_z \\ 0 & 0 & 0 & 1 \end{bmatrix}$$

(Kucuk and Bingul)

In the end-effector transformation matrix shown above,  $r_{kj}$  represents the rotational elements and  $p_x, p_y, p_z$  give the position vector (Kucuk and Bingul).

# Investigation

## Determining DH Parameters

To determine the Denavit-Hartenberg parameters, the coordinate frame assignment of the robot must first be clarified by drawing a diagram (see Figure 7).

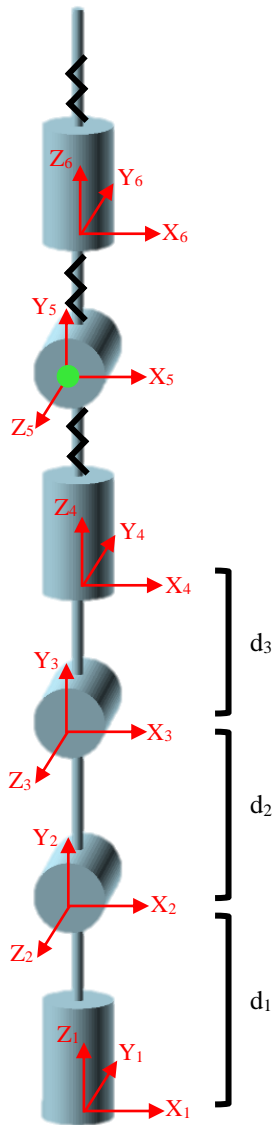


Figure 7, Coordinate frame assignment of 6 DOF manipulator

A set of axes is drawn at each of the joints. The z axes all point towards the axes of rotation, the x axes point in the same direction, and the y axes are determined with the right-hand rule.

The  $\theta_i$  for each of the joints is  $\theta_1$  through  $\theta_6$  because they are joint variables which change.

The  $a_{i-1}$  values are all zero, because there is no distance between the individual coordinate frames, along the x axes.

The  $d_i$  for the first three axes are  $d_1$  along  $Z_1$ ,  $d_2$  along  $Y_2$  and  $d_3$  along  $Y_3$ , due to the link lengths. The last three axes have  $d_i$  values equal to zero because of the Euler wrist; therefore, the position of the end-effector is taken as the green point on the figure.

And finally, the  $\alpha_{i-1}$  values must be determined. The first joint's coordinate frame is that of the base, meaning its orientation is the same as the world's, and so  $\alpha_0$  is zero. The second joint is rotated by 90 degrees counterclockwise around the x axis, so  $\alpha_1$  is 90. The third joint is in the same direction as the second, so  $\alpha_2$  is zero. The fourth joint becomes upright again, through a 90 degree clockwise rotation, so  $\alpha_3$  is -90. Similarly,  $\alpha_4$  is 90 and  $\alpha_5$  is -90.

<b>i</b>	<b><math>\theta_i</math></b>	<b><math>\alpha_{i-1}</math></b>	<b><math>d_i</math></b>	<b><math>a_{i-1}</math></b>
1	$\theta_1$	0	$d_1$	0
2	$\theta_2$	90	$d_2$	0
3	$\theta_3$	0	$d_3$	0
4	$\theta_4$	-90	0	0
5	$\theta_5$	90	0	0
6	$\theta_6$	-90	0	0

Table 2, DH parameters of 6 DOF manipulator

## Forward Kinematics

The DH parameters in Table 2 for each of the joints can then be substituted into Equation 1, yielding the individual transformation matrices. For example, the transformation matrix for the first joint is:

$${}^0_1T = \begin{bmatrix} 1 & 0 & 0 & 0 \\ 0 & c(0) & -s(0) & 0 \\ 0 & s(0) & c(0) & 0 \\ 0 & 0 & 0 & 1 \end{bmatrix} \begin{bmatrix} 1 & 0 & 0 & 0 \\ 0 & 1 & 0 & 0 \\ 0 & 0 & 1 & 0 \\ 0 & 0 & 0 & 1 \end{bmatrix} \begin{bmatrix} c(\theta_1) & -s(\theta_1) & 0 & 0 \\ s(\theta_1) & c(\theta_1) & 0 & 0 \\ 0 & 0 & 1 & 0 \\ 0 & 0 & 0 & 1 \end{bmatrix} \begin{bmatrix} 1 & 0 & 0 & 0 \\ 0 & 1 & 0 & 0 \\ 0 & 0 & 1 & d_1 \\ 0 & 0 & 0 & 1 \end{bmatrix} \\ = \begin{bmatrix} c(\theta_1) & -s(\theta_1) & 0 & 0 \\ s(\theta_1) & c(\theta_1) & 0 & 0 \\ 0 & 0 & 1 & d_1 \\ 0 & 0 & 0 & 1 \end{bmatrix}$$

The transformation matrix for the second joint can also be found similarly. Note that the  $D_x(a_{i-1})$  matrix responsible for translations along the x axis has been omitted, because that transformation isn't necessary for the given robot, and its matrix is simply an identity matrix. Additionally, the  $d_2$  variable in the  $Q_i$  translation matrix has been placed in the  $p_y$  element instead of  $p_z$ , because unlike the first joint, the translation is now along the given joint's y axis.

$${}^1_2T = \begin{bmatrix} 1 & 0 & 0 & 0 \\ 0 & c(90) & -s(90) & 0 \\ 0 & s(90) & c(90) & 0 \\ 0 & 0 & 0 & 1 \end{bmatrix} \begin{bmatrix} c(\theta_2) & -s(\theta_2) & 0 & 0 \\ s(\theta_2) & c(\theta_2) & 0 & 0 \\ 0 & 0 & 1 & 0 \\ 0 & 0 & 0 & 1 \end{bmatrix} \begin{bmatrix} 1 & 0 & 0 & 0 \\ 0 & 1 & 0 & d_2 \\ 0 & 0 & 1 & 0 \\ 0 & 0 & 0 & 1 \end{bmatrix} = \begin{bmatrix} c(\theta_2) & -s(\theta_2) & 0 & -d_2 * s(\theta_2) \\ 0 & 0 & -1 & 0 \\ s(\theta_2) & c(\theta_2) & 0 & d_2 * c(\theta_2) \\ 0 & 0 & 0 & 1 \end{bmatrix}$$

The same reasoning is applied to the other joints:

$${}^2_3T = \begin{bmatrix} c(\theta_3) & -s(\theta_3) & 0 & 0 \\ s(\theta_3) & c(\theta_3) & 0 & 0 \\ 0 & 0 & 1 & 0 \\ 0 & 0 & 0 & 1 \end{bmatrix} \begin{bmatrix} 1 & 0 & 0 & 0 \\ 0 & 1 & 0 & d_3 \\ 0 & 0 & 1 & 0 \\ 0 & 0 & 0 & 1 \end{bmatrix} = \begin{bmatrix} c(\theta_3) & -s(\theta_3) & 0 & -d_3 * s(\theta_3) \\ s(\theta_3) & c(\theta_3) & 0 & d_3 * c(\theta_3) \\ 0 & 0 & 1 & 0 \\ 0 & 0 & 0 & 1 \end{bmatrix}$$

$${}^3_4T = \begin{bmatrix} 1 & 0 & 0 & 0 \\ 0 & c(-90) & -s(-90) & 0 \\ 0 & s(-90) & c(-90) & 0 \\ 0 & 0 & 0 & 1 \end{bmatrix} \begin{bmatrix} c(\theta_4) & -s(\theta_4) & 0 & 0 \\ s(\theta_4) & c(\theta_4) & 0 & 0 \\ 0 & 0 & 1 & 0 \\ 0 & 0 & 0 & 1 \end{bmatrix} = \begin{bmatrix} c(\theta_4) & -s(\theta_4) & 0 & 0 \\ 0 & 0 & 1 & 0 \\ -s(\theta_4) & -c(\theta_4) & 0 & 0 \\ 0 & 0 & 0 & 1 \end{bmatrix}$$

$${}^4_5T = \begin{bmatrix} 1 & 0 & 0 & 0 \\ 0 & c(90) & -s(90) & 0 \\ 0 & s(90) & c(90) & 0 \\ 0 & 0 & 0 & 1 \end{bmatrix} \begin{bmatrix} c(\theta_5) & -s(\theta_5) & 0 & 0 \\ s(\theta_5) & c(\theta_5) & 0 & 0 \\ 0 & 0 & 1 & 0 \\ 0 & 0 & 0 & 1 \end{bmatrix} = \begin{bmatrix} c(\theta_5) & -s(\theta_5) & 0 & 0 \\ 0 & 0 & -1 & 0 \\ s(\theta_5) & c(\theta_5) & 0 & 0 \\ 0 & 0 & 0 & 1 \end{bmatrix}$$

$${}^5_6T = \begin{bmatrix} 1 & 0 & 0 & 0 \\ 0 & c(-90) & -s(-90) & 0 \\ 0 & s(-90) & c(-90) & 0 \\ 0 & 0 & 0 & 1 \end{bmatrix} \begin{bmatrix} c(\theta_6) & -s(\theta_6) & 0 & 0 \\ s(\theta_6) & c(\theta_6) & 0 & 0 \\ 0 & 0 & 1 & 0 \\ 0 & 0 & 0 & 1 \end{bmatrix} = \begin{bmatrix} c(\theta_6) & -s(\theta_6) & 0 & 0 \\ 0 & 0 & 1 & 0 \\ -s(\theta_6) & -c(\theta_6) & 0 & 0 \\ 0 & 0 & 0 & 1 \end{bmatrix}$$



Finally, all of the transformation matrices are multiplied to find the transformation matrix describing the end-effector's position and rotation:

$${}^0_6T = {}^0_1T * {}^1_2T * \dots * {}^5_6T = \begin{bmatrix} r_{11} & r_{12} & r_{13} & p_x \\ r_{21} & r_{22} & r_{23} & p_y \\ r_{31} & r_{32} & r_{33} & p_z \\ 0 & 0 & 0 & 1 \end{bmatrix}$$

$$= \begin{bmatrix} \dots & \dots & \dots & -d_3(c\theta_1 * c\theta_2 * s\theta_3 + c\theta_1 * c\theta_3 * s\theta_2) - d_2 * c\theta_1 * s\theta_2 \\ \dots & \dots & \dots & -d_3(c\theta_2 * s\theta_1 * s\theta_3 + c\theta_3 * s\theta_1 * s\theta_2) - d_2 * s\theta_1 * s\theta_2 \\ \dots & \dots & \dots & d_1 + d_2 * c\theta_2 + d_3(c\theta_2 * c\theta_3 - s\theta_2 * s\theta_3) \\ 0 & 0 & 0 & 1 \end{bmatrix}$$

### Verification of Model

To verify the correctness of this mathematical model, a sanity check should be performed by finding the zero position vector (the position when all the angles are zero):

$$\begin{bmatrix} p_x \\ p_y \\ p_z \end{bmatrix} = \begin{bmatrix} -d_3(c(0) * c(0) * s(0) + c(0) * c(0) * s(0)) - d_2 * c(0) * s(0) \\ -d_3(c(0) * s(0) * s(0) + c(0) * s(0) * s(0)) - d_2 * s(0) * s(0) \\ d_1 + d_2 * c(0) + d_3(c(0) * c(0) - s(0) * s(0)) \end{bmatrix} = \begin{bmatrix} 0 \\ 0 \\ d_1 + d_2 + d_3 \end{bmatrix}$$

This position vector clearly matches what one would expect based on Figure 7.

### Inverse Kinematics

Solving the inverse kinematics problem requires manipulating the following equation so that the unknown  $\theta_i$  variables can eventually be written in terms of  ${}^0_6T$ 's elements ( $p_x$ ,  $p_y$ ,  $p_z$  and  $r_{kj}$ ), which are given.

$${}^0_6T = {}^0_1T * {}^1_2T * {}^2_3T * {}^3_4T * {}^4_5T * {}^5_6T$$

To do this, the joint transformation matrices in the equation can be pre-multiplied, as shown below. This will yield multiple expressions which can all be used to find a solution.

$$[{}^0_1T]^{-1} * {}^0_6T = {}^1_2T * {}^2_3T * {}^3_4T * {}^4_5T * {}^5_6T$$

$$[{}^0_1T * {}^1_2T]^{-1} * {}^0_6T = {}^2_3T * {}^3_4T * {}^4_5T * {}^5_6T$$

...

$$[{}^0_1T * {}^1_2T * {}^2_3T * {}^3_4T * {}^4_5T]^{-1} * {}^0_6T = {}^5_6T$$

We will be using the second expression in this list, but the others could have been used as well.

Firstly, one of the elements of the matrices on the left and right hand sides must be set equal. We will start with the third row, fourth column element ( $p_z$ ) as it is the simplest of the three position element equations:

$$\frac{p_x * s(\theta_1)}{c(\theta_1)^2 + s(\theta_1)^2} - \frac{p_y * c(\theta_1)}{c(\theta_1)^2 + s(\theta_1)^2} = 0$$

$$p_x * s(\theta_1) - p_y * c(\theta_1) = 0$$

By using the second trigonometric equation from Table 1, the value of  $\theta_1$  can be found:

$$\theta_1 = \text{Atan2}(p_y, p_x) \text{ or } \text{Atan2}(-p_y, -p_x) \tag{Equation 2}$$

We will next evaluate the first row, fourth column elements ( $p_x$ ):

$$\frac{p_z * s(\theta_2)}{c(\theta_2)^2 + s(\theta_2)^2} - \frac{d_1 * s(\theta_2)}{c(\theta_2)^2 + s(\theta_2)^2} + \frac{p_x * c(\theta_1) * c(\theta_2)}{c(\theta_1)^2 c(\theta_2)^2 + c(\theta_1)^2 s(\theta_2)^2 + c(\theta_2)^2 s(\theta_1)^2 + s(\theta_1)^2 s(\theta_2)^2} + \frac{p_y * c(\theta_2) * s(\theta_1)}{c(\theta_1)^2 c(\theta_2)^2 + c(\theta_1)^2 s(\theta_2)^2 + c(\theta_2)^2 s(\theta_1)^2 + s(\theta_1)^2 s(\theta_2)^2} = -d_3 * s(\theta_3)$$

$$p_z * s(\theta_2) - d_1 * s(\theta_2) + p_x * c(\theta_1) * c(\theta_2) + p_y * c(\theta_2) * s(\theta_1) = -d_3 * s(\theta_3)$$

$$s(\theta_2) * [p_z - d_1] + c(\theta_2) * [p_x * c(\theta_1) + p_y * s(\theta_1)] = -d_3 * s(\theta_3)$$

$$v * s(\theta_2) + w * c(\theta_2) = -d_3 * s(\theta_3) \quad \text{where } v = p_z - d_1 \text{ and } w = p_x * c(\theta_1) + p_y * s(\theta_1) \quad \text{Equation 3}$$

Next, we will use the elements in the second row and fourth column ( $p_y$ ):

$$\frac{p_x * c(\theta_2)}{c(\theta_2)^2 + s(\theta_2)^2} - \frac{d_2 * c(\theta_2)^2 + d_2 * s(\theta_2)^2 + d_1 * c(\theta_2)}{c(\theta_2)^2 + s(\theta_2)^2} - \frac{p_x * c(\theta_1) * s(\theta_2)}{c(\theta_1)^2 c(\theta_2)^2 + c(\theta_1)^2 s(\theta_2)^2 + c(\theta_2)^2 s(\theta_1)^2 + s(\theta_1)^2 s(\theta_2)^2} - \frac{p_y * s(\theta_2) * s(\theta_1)}{c(\theta_1)^2 c(\theta_2)^2 + c(\theta_1)^2 s(\theta_2)^2 + c(\theta_2)^2 s(\theta_1)^2 + s(\theta_1)^2 s(\theta_2)^2} = d_3 * c(\theta_3)$$

$$p_x * c(\theta_2) - d_2 - d_1 * c(\theta_2) - p_x * c(\theta_1) * s(\theta_2) - p_y * s(\theta_2) * s(\theta_1) = d_3 * c(\theta_3)$$

$$c(\theta_2) * [p_x - d_1] - s(\theta_2) * [p_x * c(\theta_1) + p_y * s(\theta_1)] = d_2 + d_3 * c(\theta_3)$$

$$v * c(\theta_2) - w * s(\theta_2) = d_2 + d_3 * c(\theta_3) \quad \text{Equation 4}$$

Equations 3 and 4 can then be squared and added to find a value for  $\theta_3$ :

$$v^2 * s(\theta_2)^2 + w^2 * c(\theta_2)^2 + 2vw * s(\theta_2) * c(\theta_2) = d_3^2 * s(\theta_3)^2$$

$$v^2 * c(\theta_2)^2 + w^2 * s(\theta_2)^2 - 2vw * s(\theta_2) * c(\theta_2) = d_2^2 + d_3^2 * c(\theta_3)^2 + 2d_2 d_3 * c(\theta_3)$$

$$v^2 + w^2 = d_2^2 + d_3^2 + 2d_2 d_3 * c(\theta_3)$$

$$\theta_3 = \arccos\left(\frac{v^2 + w^2 - d_2^2 - d_3^2}{2d_2 d_3}\right)$$

$$\theta_3 = \arccos\left(\frac{[p_z - d_1]^2 + [p_x * c(\theta_1) + p_y * s(\theta_1)]^2 - d_2^2 - d_3^2}{2 * d_2 * d_3}\right) \quad \text{Equation 5}$$

This value can then be used to find  $\theta_2$ , using Equation 3 and the first trigonometric equation in Table 1.

$$v * s(\theta_2) + w * c(\theta_2) = c \quad \text{where } v = p_z - d_1, w = p_x * c(\theta_1) + p_y * s(\theta_1) \text{ and } c = -d_3 * s(\theta_3)$$

$$\theta_2 = \text{Atan2}(v, w) \pm \text{Atan2}\left(\sqrt{v^2 + w^2 - c^2}, c\right)$$

$$\theta_2 = \text{Atan2}\left(p_z - d_1, p_x * c(\theta_1) + p_y * s(\theta_1)\right) \pm \text{Atan2}\left(\sqrt{[p_z - d_1]^2 + [p_x * c(\theta_1) + p_y * s(\theta_1)]^2 - [-d_3 * s(\theta_3)]^2}, -d_3 * s(\theta_3)\right) \quad \text{Equation 6}$$

Hence, the values of  $\theta_1$ ,  $\theta_2$  and  $\theta_3$ , which are the joint angles that affect the end-effector's position, are found. The angles of the other three joints weren't explored because those aren't responsible for the end-effector's position, but rather it's orientation, which isn't as significant. However, those could also be found using the same method, with the  $r_{ij}$  elements of the matrices.

## Verification of Inverse Kinematics

The inverse kinematics solution can be verified by applying it to a position with a known joint solution. That is, if we use the forward kinematics model to calculate the position vector for a set of given joint angles, and then substitute the position vector back into the inverse kinematics expressions, we should find the original angles, along with other potential solutions (which may or may not be correct).

If the first three joint angles (which are the ones responsible for the position) are taken as 45, 30 and -90 degrees respectively, and all of the link lengths ( $d_i$  variables) are taken as 1 meter, the end-effector position vector becomes:

$$\begin{bmatrix} p_x \\ p_y \\ p_z \end{bmatrix} = \begin{bmatrix} -1 * (c(45) * c(30) * s(-90) + c(45) * c(-90) * s(30)) - 1 * c(45) * s(30) \\ -1 * (c(30) * s(45) * s(-90) + c(-90) * s(45) * s(30)) - 1 * s(45) * s(30) \\ 1 + 1 * c(30) + 1 * (c(30) * c(-90) - s(30) * s(-90)) \end{bmatrix}$$

$$= \begin{bmatrix} 0.2588190451 \\ 0.2588190451 \\ 2.366025404 \end{bmatrix}$$

This value appears reasonable, as the first joint angle is 45 degrees, and the  $p_x$  and  $p_y$  values are therefore equal.

It can then be inputted to the inverse kinematics expressions. If we use Equation 2 to find the first angle:

$$\theta_1 = \text{Atan2}(0.2588190451, 0.2588190451) \text{ or } \text{Atan2}(-0.2588190451, -0.2588190451)$$

$$\theta_1 = 45^\circ \text{ or } -135^\circ$$

Next, Equation 5 is used for the third angle. Both values of the first angle (45 and -135 degrees) are substituted into this expression, to find all possible solutions:

$$\theta_3 = \arccos\left(\frac{[2.366025404 - 1]^2 + [0.2588190451 * c(45) + 0.2588190451 * s(45)]^2 - 1^2 - 1^2}{2 * 1 * 1}\right)$$

$$= 90^\circ \text{ or } -90^\circ$$

or

$$\theta_3 = \arccos\left(\frac{[2.366025404 - 1]^2 + [0.2588190451 * c(225) + 0.2588190451 * s(225)]^2 - 1^2 - 1^2}{2 * 1 * 1}\right)$$

$$= 90^\circ \text{ or } -90^\circ$$

And lastly, Equation 6 is used to find the second angle. Once again, all combinations of the first and third angles' values are used:

$$\theta_2 = \text{Atan2}(2.366025404 - 1, 0.2588190451 * c(45) + 0.2588190451 * s(45))$$

$$\pm \text{Atan2}\left(\sqrt{[2.366025404 - 1]^2 + [0.2588190451 * c(45) + 0.2588190451 * s(45)]^2} - [-1 * s(90)]^2, -1 * s(90)\right) = -60^\circ \text{ or } -150^\circ$$

or

$$\theta_2 = \text{Atan2}(2.366025404 - 1, 0.2588190451 * c(45) + 0.2588190451 * s(45))$$

$$\pm \text{Atan2}\left(\sqrt{[2.366025404 - 1]^2 + [0.2588190451 * c(45) + 0.2588190451 * s(45)]^2} - [-1 * s(-90)]^2, -1 * s(-90)\right) = 30^\circ \text{ or } 120^\circ$$

or

$$\theta_2 = \text{Atan2}(2.366025404 - 1, 0.2588190451 * c(225) + 0.2588190451 * s(225)) \\ \pm \text{Atan2}\left(\sqrt{[2.366025404 - 1]^2 + [0.2588190451 * c(225) + 0.2588190451 * s(225)]^2 - [-1 * s(90)]^2},\right. \\ \left. - 1 * s(90)\right) = -30^\circ \text{ or } -120^\circ$$

or

$$\theta_2 = \text{Atan2}(2.366025404 - 1, 0.2588190451 * c(225) + 0.2588190451 * s(225)) \\ \pm \text{Atan2}\left(\sqrt{[2.366025404 - 1]^2 + [0.2588190451 * c(225) + 0.2588190451 * s(225)]^2 - [-1 * s(-90)]^2},\right. \\ \left. - 1 * s(-90)\right) = 60^\circ \text{ or } 150^\circ$$

As shown, the 45, 30 and -90 degree joint configuration is indeed one of the potential solutions yielded by the inverse kinematics. This indicates that the inverse kinematics solution is correct.

Note that when using the inverse kinematics with new and unknown positions, after all of the possible joint angles are found, they must be checked through the forward kinematics expression to find which angle combinations yield correct results.

## Conclusion

In this investigation, the inverse kinematics solution of a 6 DOF articulated robot has been derived algebraically, using homogenous transformation matrices. This is a significant finding in the area of automated robotics, because it allows for the autonomous control of industrial robots by supplying only the desired end-effector positions, instead of the traditional method of manually programming each of the necessary joint angles.

It should be kept in mind that the angle values yielded by the solution above need to be validated, based on two things: whether they are within the joint's physical constraints, and whether they actually move the end-effector to the target position. The first can be verified by checking the solution against a domain for the angle, and the second by substituting the values into the forward kinematics expression found on page 9. Therefore, it can be concluded that not all of the solutions will be valid, and that they must be checked manually or through a computer program.

Furthermore, the inverse kinematics solution explored above can't handle singularities. These are cases when there are infinite solutions. For example, when the robot is in its zero position (all angles are zero, so the robot points upwards), even though  $\theta_2$  must be zero,  $\theta_1$  and  $\theta_3$  can be an infinite number of values. That's why when one tries to use the inverse kinematics formulas to find the solution to  $\theta_1$ ,  $\tan(0)$  is found, which is undefined.

And finally, the robot being investigated had a Euler wrist, which is certainly not the case for many 6 DOF industrial robots. This means that this solution, like many others in literature, have a limited scope of applicability. In the future, this could be expanded by examining other methods of inverse kinematics that don't involve position and orientation decoupling through the Euler wrist.

This mathematical investigation has taught me about robot design, modelling and kinematics. I have learned about Denavit-Hartenberg parameters and how they can be used with homogenous transformation matrices, which is a common practice in robotics research and literature. I have also gained an appreciation for transformation matrices, as I have noticed how convenient and powerful they can be. This investigation, along with my extended essay on robot design, have been great opportunities for me to explore my passion for robotics. I wish to pursue education in similar topics during my future University education.

## Works Cited

DENSO WAVE INCORPORATED. "Joint Mode (6-axis Robot)." n.d. *DENSO Robot User Manuals*.

FANUC. "R-2000iC/270F industrial robot." n.d. *FANUC Europe Corporation*.

Kucuk, Serdar and Zafer Bingul. "Robot Kinematics: Forward and Inverse Kinematics." Cubero, Sam. *Industrial Robotics: Theory, Modelling and Control*. InTech, 2006.  
<[http://www.intechopen.com/books/industrial\\_robotics\\_theory\\_modelling\\_and\\_control/robot\\_kinematics\\_\\_forward\\_and\\_inverse\\_kinematics](http://www.intechopen.com/books/industrial_robotics_theory_modelling_and_control/robot_kinematics__forward_and_inverse_kinematics)>.

Ross, Larry, et al. *Robotics: Theory and Industrial Applications*. Goodheart-Willcox, 2010.  
<[http://www.g-w.com/pdf/sampchap/9781605253213\\_ch02.pdf](http://www.g-w.com/pdf/sampchap/9781605253213_ch02.pdf)>.

Szabó, Zsolt, et al. "4. fejezet - Példák – Tipikus nyítláncú robotkarok." 2014. *Robotmechanizmusok*.

Yetim, Coşkun. *Kinematic Analysis for Robot Arm*. Istanbul: Yıldız Technical University, 2009.